AMERICAN SOCIETY FOR MICROBIOLOGY | Journal of Virology®

VACCINES AND ANTIVIRAL AGENTS

An HIV Vaccine Targeting the V2 Region of the HIV Envelope Induces a Highly Durable Polyfunctional Fc-Mediated Antibody Response in Rhesus Macaques

Rebecca L. Powell,[a] Svenja Weiss,[a] Alisa Fox,[a] Xiaomei Liu,[a] Vincenza Itri,[a] Xunqing Jiang,[b] Christina C. Luo,[b] David A. Spencer,[c] Shilpi Pandey,[c] Tracy Cheever,[c] Deborah H. Fuller,[d,e] Maxim Totrov,[f] Ann J. Hessell,[c] Nancy L. Haigwood,[c,e] Xiang-Peng Kong,[b] Susan Zolla-Pazner[a]

[a]Department of Medicine, Division of Infectious Diseases, Icahn School of Medicine at Mount Sinai, New York, New York, USA
[b]Department of Biochemistry and Molecular Pharmacology, NYU School of Medicine, New York, New York, USA
[c]Division of Pathobiology and Immunology, Oregon National Primate Research Center, Oregon Health and Science University, Beaverton, Oregon, USA
[d]Department of Microbiology, University of Washington School of Medicine, Seattle, Washington, USA
[e]Washington National Primate Research Center, Seattle, Washington, USA
[f]Molsoft LLC, La Jolla, California, USA

ABSTRACT The HIV vaccine field now recognizes the potential importance of generating polyfunctional antibodies (Abs). The only clinical HIV vaccine trial to date to show significant efficacy (RV144) found that reduced infection rates correlated with the level of nonneutralizing Abs specific for the V2 region of the envelope glycoprotein. We have conducted a comprehensive preclinical reverse vaccinology-based vaccine program that has included the design and production and testing of numerous scaffolded V2 region immunogens. The most immunogenic vaccine regimen in nonhuman primates among those studied as part of this program consisted of a cocktail of three immunogens presenting V2 from different viruses and clades in the context of different scaffolds. Presently we demonstrate that the V2-specific Ab response from this regimen was highly durable and functionally diverse for the duration of the study (25 weeks after the final immunization). The total IgG binding response at this late time point exhibited only an ~5× reduction in potency. Three immunizations appeared essential for the elicitation of a strong Ab-dependent cellular cytotoxicity (ADCC) response for all animals, as opposed to the Ab-dependent cellular phagocytosis (ADCP) and virus capture responses, which were comparably potent after only 2 immunizations. All functionalities measured were highly durable through the study period. Therefore, testing this vaccine candidate for its protective capacity is warranted.

IMPORTANCE The only HIV vaccine trial for which protective efficacy was detected correlated this efficacy with V2-specific Abs that were effectively nonneutralizing. This result has fueled a decade of HIV vaccine research focused on designing an HIV vaccine capable of eliciting V2-focused, polyfunctional Abs that effectively bind HIV and trigger various leukocytes to kill the virus and restrict viral spread. From the numerous vaccine candidates designed and tested as part of our V2-focused preclinical vaccine program, we have identified immunogens and a vaccine regimen that induces a highly durable and polyfunctional V2-focused Ab response in rhesus macaques, described herein.

KEYWORDS Fc mediated, HIV, V2 loop, vaccine, antibody, rhesus macaque

The only clinical human immunodeficiency virus (HIV) vaccine trial to date to show significant efficacy (RV144) found that reduced infection rates correlated with the level of nonneutralizing antibodies (Abs) specific for the V2 region of the gp120

Citation Powell RL, Weiss S, Fox A, Liu X, Itri V, Jiang X, Luo CC, Spencer DA, Pandey S, Cheever T, Fuller DH, Totrov M, Hessell AJ, Haigwood NL, Kong X-P, Zolla-Pazner S. 2020. An HIV vaccine targeting the V2 region of the HIV envelope induces a highly durable polyfunctional Fc-mediated antibody response in rhesus macaques. J Virol 94:e01175-20. https://doi.org/10.1128/JVI.01175-20.

Editor Guido Silvestri, Emory University

Address correspondence to Rebecca L. Powell, Rebecca.Powell@mssm.edu.

Received 11 June 2020
Accepted 13 June 2020
Accepted manuscript posted online 17 June 2020
Published 17 August 2020

envelope (Env) glycoprotein, and this finding was extended to show a correlate with V2-reactive IgG3 Abs (1–4). Many Abs that are capable of binding to the surfaces of viruses or virus-infected cells can facilitate a variety of activities that contribute to viral clearance, mediated by the "constant" region of the immunoglobulin molecule—the crystallizable fragment (Fc)—via interactions with Fc receptors (FcRs) found on virtually all innate immune cells, linking the Abs elicited by the adaptive immune response with innate immune functions (5). The HIV vaccine field now recognizes the potential importance of generating Fc-functional Abs, realizing that "both ends" of an Ab are critical components of the biologic functions they mediate, and consequently, there is now an appreciation of the need to design vaccines capable of eliciting Abs that can trigger relevant leukocytes via FcRs to destroy virus, kill infected cells, and restrict viral spread. Follow-up analyses of the RV144 data found that Fc-mediated activities, including Ab-dependent cellular cytotoxicity (ADCC) and Ab-dependent cellular phagocytosis (ADCP), correlated with the level of serum V2 Abs (6–10), consistent with previous studies implicating Fc-mediated Ab activities in the response to various pathogens (11–16). Data from various nonhuman primate (NHP) studies strongly support the idea that vaccine-induced Abs specific for the V2 domain control viremia and/or reduce the risk of infection (17–22).

The V2 Env domain is characterized by four epitope families—V2p, V2i, V2q, and V2qt— defined by numerous human monoclonal Abs (MAbs) isolated over the past 3 decades. V2p epitopes are defined by human MAbs that bind strongly to linear peptides and are nonneutralizing (23, 24). V2i epitopes are discontinuous and overlay the $\alpha 4\beta 7$ integrin binding site, and V2i MAbs are only weakly neutralizing but can effectively elicit Fc-mediated functions (9, 25–29). V2q epitopes prefer native/native-like trimeric Env structures and are defined by a group of broadly neutralizing Abs (bNAbs), such as PG9 and PG16 (30, 31). V2qt epitope family MAbs are trimer dependent, binding at the Env trimer's axial center, and characterized by broad and potent neutralizing activity; this family includes PGT145 and PGDM1400 (32, 33).

We have conducted a comprehensive reverse vaccinology-based vaccine program in rabbits and NHPs that has included the design and production and testing of numerous scaffolded V2 domain immunogens derived from HIV-1 isolates from clades A, B, and C (34, 35). These have successfully focused the Ab response on V2 and induced cross-clade reactive and biologically active V2 Abs (35). Most recently, we have reported the ability of these scaffolded V2 immunogens, in combination with DNA gp120 immunization, to elicit V2-specifc Abs in NHPs that exhibit preferential binding to trimer-like V2 Env antigens and mediate ADCC and ADCP (36). In a comprehensive study of immunogenicity in NHPs, several V2-scaffolded proteins and vaccine regimens were compared, with one vaccine group, group 7, exhibiting the strongest and most consistent activity. This group of monkeys was immunized with three scaffolded immunogens, including V1V2(ZM53)-2F5K (clade C) and V1V2(A244)-2J9C (clade E), which were designed to mimic the trimeric V2 at the apex of the prefusion Env trimer (37–40), as well as V1V2(ZM109)-TTB (clade C), developed because the typhoid toxin B (TTB) scaffold self-assembles into pentamers, presents five copies of the V2 domain, binds to cell surface gangliosides, induces mucosal immunity, and possesses a structural site compatible for the engraftment of a disulfide loop compatible with that at the base of V2 in an immunologically accessible configuration (34, 41).

Plasma Abs in group 7 NHPs demonstrated the best overall immune reactivity, including binding to various V2 antigens, neutralization of a heterologous tier 1B clade C virus, displaying increasing avidity over the course of the immunization, and mediating V2-directed ADCP as well as ADCC killing of simian-human immunodeficiency virus (SHIV)-infected cells (36). Consequently, we aimed in the present study to examine the Ab response of this group of NHPs more comprehensively and longitudinally over a period that included three immunizations and a total of 45 weeks of follow-up, measuring several parameters of immunologic activity.

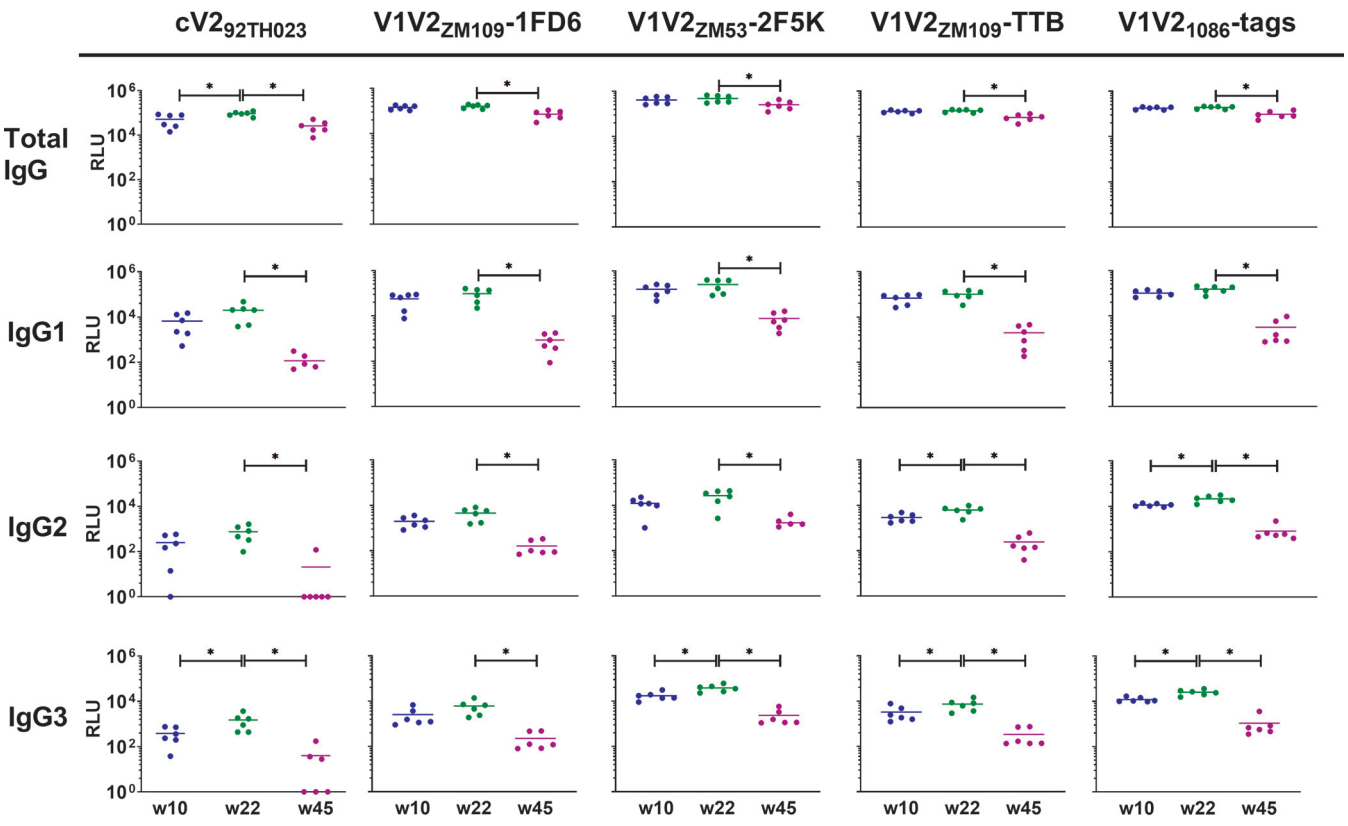

FIG 1 Plasma IgG binding to various V2 antigens. Fluorescence was measured using a Luminex FlexMAP3D device. Means from duplicate experiments with SEM of the relative light unit (RLU) readout at 1/50 plasma dilution are shown. Values for weeks 10 and 22 were measured 2 weeks after the 2nd and 3rd immunizations, respectively. *, $P < 0.05$.

RESULTS

Luminex multiplex binding assays exhibited high V2-specific titers after 2 immunizations and good durability over the study period. Data were generated simultaneously against six antigen-coupled bead types with plasma from each time point. Antigens tested included a relatively constrained, monomeric V2 domain from clade C isolate ZM109 in the context of the 1FD6 scaffold (V1V2ZM109-1FD6) (34, 36), a relatively constrained V2 domain from clade C isolate ZM53 presented as a trimer on the 2F5K scaffold (V1V2ZM53–2F5K), a relatively constrained V2 domain from clade C isolate ZM109 presented as a pentamer on the TTB scaffold (V1V2$_{ZM109}$-TTB), a relatively unconstrained V2 domain from clade C isolate 1086 in the context of C-terminal His and Avi tags (V1V2$_{1086}$-tags) (23), and a relatively unconstrained cyclic V2 peptide from clade E isolate 92TH023 (cV2$_{92TH023}$) (42). Bovine serum albumin (BSA)-coated beads and prebleed NHP plasma were used as negative controls. Notably, cV2$_{92TH023}$ and V2$_{1086}$-tags are heterologous to the immunogens used for this animal group. Total IgG, IgG1, IgG2, and IgG3 reactive to each antigen were measured at 4 plasma dilutions. Measurements at 1/50 plasma dilution are shown in Fig. 1 and are representative of titration curves (see Fig. S1a to d in the supplemental material). As previously reported, total IgG in plasma from the immunized animals was highly reactive to all five V2 antigens tested at week 22, 2 weeks after the final immunization (Fig. 1, first row). Notably, 2 weeks after the 2nd immunization (at week 10), total IgG specific for 4/5 antigens measured was already just as potent, with no significant differences in specific titer between weeks 10 and 22 (unpaired Mann-Whitney test). Only reactivity to cV2$_{92TH023}$ appeared to significantly increase after the final immunization (Fig. 1; $P = 0.026$). In terms of IgG1-specific Abs, no boosting effect against any of the antigens tested was observed after the final immunization (Fig. 1, second row). IgG2-specific Abs were only significantly boosted against V1V2$_{1086}$-tags and V1V2$_{ZM109}$-TTB by the final

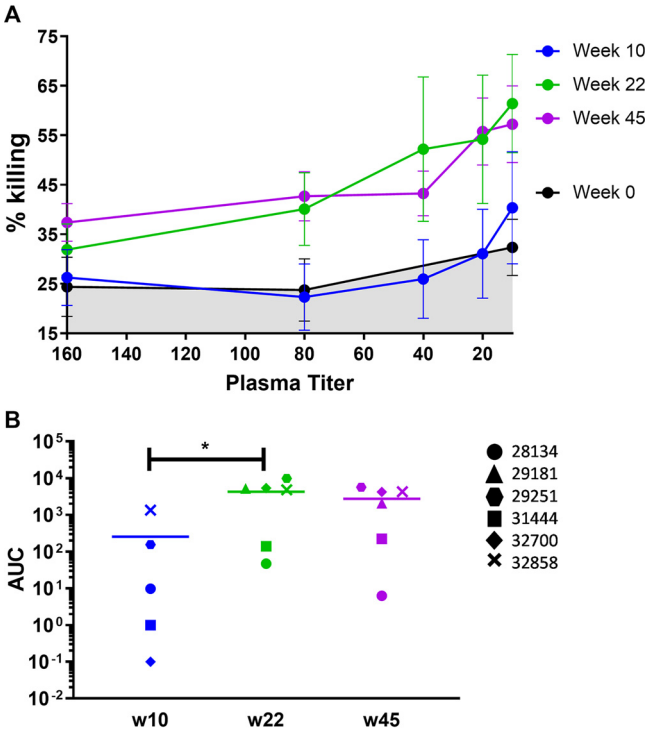

FIG 2 ADCC activity in NHP plasma. (A) Percent killing at each plasma dilution compared to the no-plasma control wells. Means from duplicate assays with SEM are shown. (B) The AUC of each titration curve was calculated. *, $P < 0.05$.

immunization (Fig. 1, third row, $P = 0.0087$ and 0.0152, respectively), while this final boost significantly improved IgG3 titers against all antigens but V1V2ZM109-1FD6 (Fig. 1, fourth row, $P = 0.0042$ to 0.0411).

In all cases, the total IgG V2-reactive Ab response against all antigens measured was durable and persisted at the latest time point measured (45 weeks after the first immunization, which was 25 weeks after the final boost; Fig. 1, first row). Although the reactivity at 1/50 plasma dilution was significantly reduced by week 45, the mean decrease was $<5\times$ in all cases ($P = 0.0022$ to 0.026). IgG1 reactivity at week 45 significantly decreased against all antigens $\sim 10\times$ to 100x compared to week 22 ($P = 0.0022$; Fig. 1, s row), while IgG2 reactivity generally decreased $\sim 5\times$ to $10\times$ ($P = 0.0022$ to 0.0043; Fig. 1, third row). Notably, no IgG2 reactivity to $cV2_{92TH023}$ was measurable above background at week 45 for 5/6 animals. IgG3 reactivity decreased $\sim 10\times$ for all antigens, with no IgG3 reactivity to $cV2_{92TH023}$ apparent for 3/6 animals at this time point ($P = 0.0022$; Fig. 1, fourth row).

ADCC activity against $SHIV_{SF162P3}$-infected target cells required 3 immunizations but remained highly durable over the study period. The ability of the vaccine-induced Abs to mediate killing of SHIV-infected cells was analyzed and compared using plasma from the six immunized NHPs 2 weeks after the 2nd and 3rd immunizations (weeks 10 and 22) and 25 weeks after the last immunization (week 45). Percent killing was determined and the area under the concentration-time curve (AUC) of the titration curves calculated. After the 2nd immunization, there was a wide range of responses among the 6 animals; only 2 of 6 animals exhibited ADCC activity at this time point, with 30–50% killing at the highest concentration of plasma tested (Fig. 2). Two weeks after the final immunization, a significant boost in ADCC activity was observed ($P = 0.0238$; unpaired Mann-Whitney test), with animals exhibiting a peak mean killing of 64% (range: 34% to 94% [Fig. 2] [36]). These responses were highly durable. There was no significant decline in mean ADCC activity between weeks 22 and 45 despite no further immunizations occurring. Indeed, three of the animals exhibited increased levels of killing (Fig. 2B).

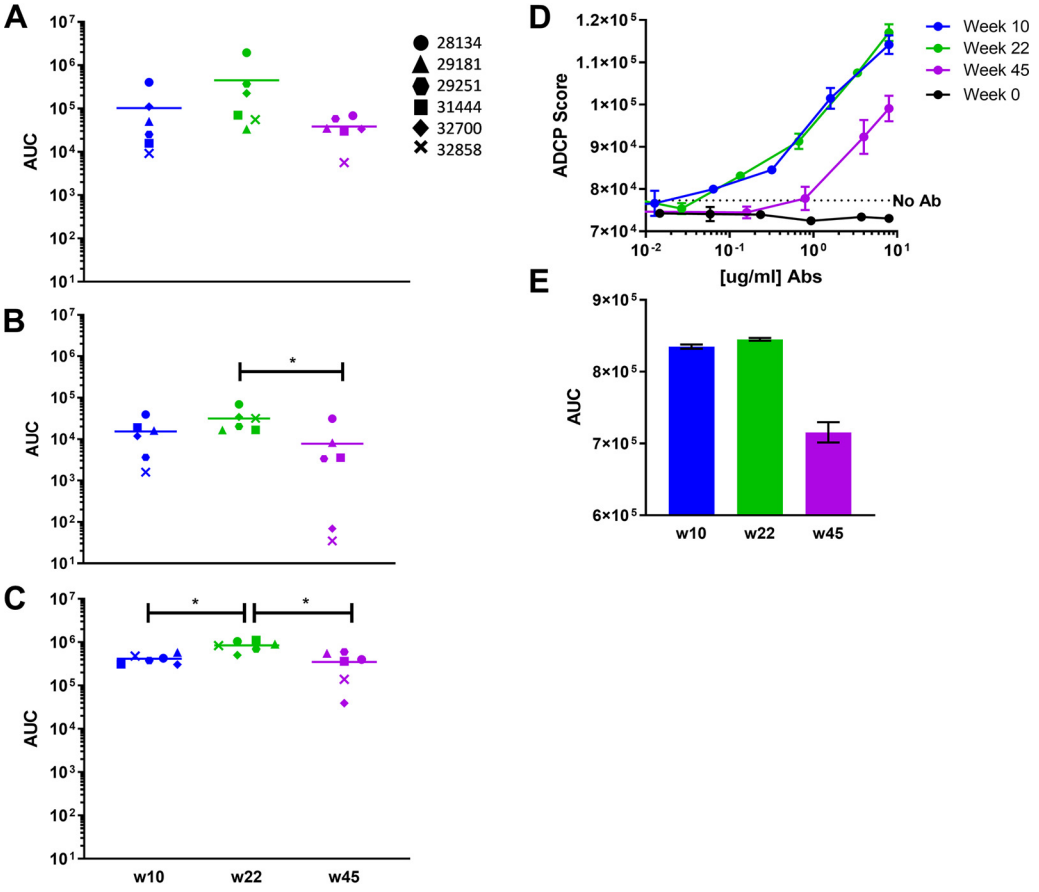

FIG 3 ADCP activity in NHP plasma. (A to C) ADCP of beads conjugated to V2(ZM109)-1FD6 (A), V2(ZM53)-2F5K (B), or V2(ZM109)-TTB (C). ADCP was measured on an LSR Fortessa. ADCP scores at each plasma dilution were used to generate titration curves, from which AUCs were calculated. (D and E) Virus-based ADCP elicited by V2 affinity-purified Ab from pooled plasma. Means from triplicate assays are shown with SEM. *, $P < 0.05$.

ADCP activity against V2-coated microbeads and HIV particles was potent after 2 immunizations and durable over the study period. Plasma from each time point was assayed for the ability to elicit ADCP of 1-μm microbeads conjugated to either V1V2(ZM109)-1FD6, V1V2(ZM53)-2F5K, or V1V2(ZM109)-TTB. ADCP was measured using human THP-1 cells. ADCP scores were calculated for each plasma dilution, generating titration curves from which AUC values were determined. Activity against all three antigens was already potent after the 2nd immunization for all animals and only 5$\times$ to 10x lower than the peak response observed at week 22 after the final immunization (Fig. 3A to C). The final boost elicited a significant increase only in the uptake of V1V2(ZM109)-TTB beads (Fig. 3C) ($P = 0.0043$; unpaired Mann-Whitney test). ADCP was durable through the last measurement at week 45, though an ~5 to 50$\times$ reduction in activity was observed. This decrease was not significant against V1V2(ZM109)-1FD6-coated beads (Fig. 3A). ADCP of V1V2(ZM53)-2F5K and V1(ZM109)-TTB-coated beads did decrease significantly ($P= 0.0152$ and $P= 0.0087$, respectively; unpaired Mann-Whitney test).

NHP plasma samples from each time point were pooled and used to purify V2-specific Abs on a V1V2(ZM109)-1FD6-agarose affinity column. Consistent with the Luminex data (Fig. 1), the largest amount of V2-specific Ab was purified 2 weeks after the final immunization at week 22 (data not shown). From 500 μl of plasma pooled from animals at weeks 10, 22, and 45, 11.7, 16.7, and 5.2 μg of V2-specific Ab were recovered from the columns, respectively. This purified protein was adjusted to the same concentration and used to assess ADCP by THP-1 cells of clade B HIV-GFP$_{11058}$

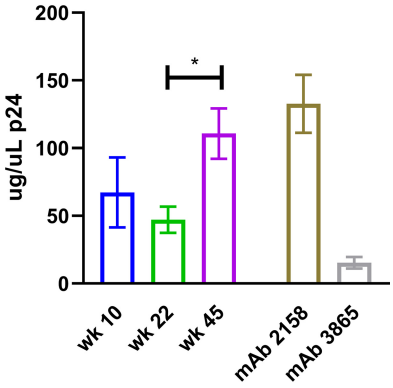

FIG 4 Capture of HIV_{ZM53} pseudoviruses by V2 affinity-purified plasma antibodies. p24 quantities of the captured virus were interpolated from a standard p24 curve. Values shown were obtained using 0.056 μg/ml of V2 affinity-purified Ab, which yielded peak virus capture as determined from the titration curve. Means from triplicate experiments with SEM are shown. *, $P < 0.05$.

virions, which are heterologous to the immunogens. Notably, week 10 and week 22 samples exhibited very similar phagocytosis of virions which was significantly above background levels (Fig. 3D). At week 45, ADCP activity was decreased by only ~20% compared to that at week 22 (Fig. 3E).

Capture activity of homologous HIV pseudovirus was potent after 2 immunizations and extremely durable over the study period. The V2-affinity-purified material from pooled plasma at each time point was also assayed for its ability to capture HIV_{ZM53} pseudoviruses, which are homologous to the V1V2(ZM53)-2F5K immunogen. Captured virions were lysed and quantified using a p24 enzyme-linked immunosorbent assay (ELISA). As seen in Fig. 4, the capacity of the V2-affinity-purified plasma Abs for virus capture was similar after the 2nd and 3rd immunizations (47 to 67 μg/μl of p24). Unlike other measurements of Ab function, at week 45 the capacity of the V2-purified material to capture virus was significantly higher than at week 22 (111 μg/μl p24 captured; $P = 0.029$, unpaired Mann-Whitney test). The increased capture functionality at week 45 was also apparent when comparing titration curves, with week 45 exhibiting an AUC ~2-fold greater than previous time points ($P = 0.029$). The amount of virus captured with V2-affinity-purified plasma Abs from weeks 10, 22, and 45 were all similar to that captured by the positive-control V2i-specific MAb 2158 at the same concentration.

DISCUSSION

A robust Ab response specific for the V2 region of HIV gp120, capable of eliciting Fc-mediated antiviral function, has been shown to correlate with reduced HIV infection risk (1–4). A similar Ab response has been shown to reduce the risk of simian immunodeficiency virus (SIV) and SHIV infection and dissemination (19, 20, 22). Therefore, there is ample evidence arguing in favor of a V2-epitope-targeted vaccine aimed at eliciting specific Abs with antiviral functions. We have rationally designed immunogens that focus the Ab response on V2, scaffolding the V1V2 loop such that V2 structure is maintained in a manner highly similar to that of the Env trimer, as demonstrated by reactivity with a panel of V2-specific MAbs (34–36). The most immunogenic vaccine regimen in NHPs among those studied consisted of a cocktail of three V2-scaffold immunogens presenting V2 from different viruses and clades in the context of different scaffolds. Of those tested, this regimen was superior for induction of antiviral responses in NHPs in terms of Ab binding, mucosal targeting, neutralization, and Fc-effector functions, while increasing affinity with each immunization and exhibiting the highest affinity (lowest off-rate) 2 weeks after the last immunization (36).

In the present study, we demonstrated that the V2-specific Ab response induced by the cocktail of immunogens was highly durable and functionally diverse for the study (25 weeks after the final immunization). When examining the total IgG response, only

2 immunizations appeared necessary for maximum binding potency for all antigens assayed except against the cyclic V2 peptide included in the multiplex analysis. This antigen is reactive only with V2p-type MAbs (35). As the animals in the vaccine study group investigated in this study were immunized with trimeric and pentameric constrained V2 immunogens that react with V2i-type MAbs, the slower Ab response to the V2p-type antigen is not surprising. The final immunization appeared critical for a broad V2 IgG2 and IgG3 response but not for the IgG1 response. The overall total IgG binding response was quite durable by week 45, with only an ~5× reduction in potency. However, IgG1 specifically appeared to wane the most, with 10× to 100× reductions in the binding response being observed. The IgG2 and IgG3 response decreased ~5× to 10×, with reactivity to the V2p-type antigen $cV2_{92TH023}$ appearing to wane most significantly. As the total IgG response appeared to have waned much less than the specific IgG1, 2, and 3 responses, it may be that much of the IgG at week 45 is IgG4, which could not be measured due to a lack of specific reagents. Macaque IgG isotypes are less diverse than those found in humans; for example, human IgG3 possesses a very long hinge region, while no analog exists among any macaque species (43). As with humans, IgG1 through IgG4 are numbered according to serum prevalence, but macaque IgG functions, including ADCC, ADCP, and FcR binding, are relatively more consistent across the IgG isotypes (44). It is generally not well understood what the observed polymorphisms among the macaque IgG isotypes signify, though repetitive vaccine boosts have been found to increase IgG4 magnitude (43). The present study in NHPs may have no bearing in terms of the potential IgG isotypes elicited by our immunogens in humans; however, this study does highlight that over the course of immunization, these isotypes may change and until the clinical phase, and this cannot be reliably predicted or well understood.

The final immunization appeared essential for the elicitation of a strong ADCC response for all animals, as opposed to the ADCP response, which was already potent after the 2nd immunization for all animals. Both ADCC and bead ADCP were highly durable at week 45, with no decline in ADCC activity and only an ~5× to 10× reduction in ADCP activity. As well, using V2-affinity purified plasma Abs, highly comparable levels of virus ADCP were observed after the 2nd and 3rd immunizations, a level of activity which was similarly durable at week 45. This V2-affinity-purified material also captured virus comparably after the 2nd and 3rd immunizations, and not only did this function persist over time, but also an increased capacity for virus capture was exhibited at week 45. It appears from these data that although all function requires binding to viruses or infected cells, not all binding will necessarily elicit the same function. A heightened ability at week 45 to capture virus was observed using V2-specific antibody affinity-purified plasma. This increased binding capacity was not apparent in the Luminex binding data. This may have been due to the use of plasma versus affinity-purified antibody, and/or binding differences in antigen coating beads versus antigen displayed on the viral surface. Furthermore, there was no comparable increase in virus ADCP activity at week 45. This may have been due to the fact that the virus targets were not the same in these assays (the HIV-green fluorescent protein [GFP] used for ADCP was a clade B virus found to be optimal in this assay; ZM53/clade C virus with a GFP tag was not available for testing). As well, the target for virus capture was pseudovirus and therefore likely expressed more surface Env, possibly increasing the effective binding capacity; however, this would not explain the relative increase in activity at week 45 (45).

The immunogens used as a vaccine in this study, which comprise our optimal vaccine candidate, induce a highly durable and polyfunctional V2-focused Ab response. The data suggest that 3 immunizations were essential for eliciting a broad, robust, and complete Ab response, though a potent response was induced even after 2 immunizations. Further study as to the particular roles and importance of each NHP IgG isotype is needed for a complete picture of this vaccine's immunogenicity. Testing the effectiveness of this vaccine's response in protection from infection is a critical next step and should include assessment not only immediately following the final immunization but also at various time points months or years after the vaccine regimen is administered.

MATERIALS AND METHODS

Immunogen preparation. Codon-optimized gp120 DNA was prepared in the pJW4303 vector with a tissue plasminogen activator (tPA) leader sequence, as described previously (46, 47). The genes of the following proteins were used to prepare the scaffolds of the V2-scaffold immunogens: PDB accession numbers 4K6L (TTB) (48), 2J9C (49), and 2F5K (50). The V2 sequences of the full-length V2 regions used as inserts into the scaffolds were previously provided (34). Genes of the V2 scaffolds were chemically synthesized and cloned into the pVRC8400 plasmid, followed by expression in HEK293 GnTI$^{-/-}$cells and purification by affinity chromatography (51). Details of the design and construction of the immunogens are described separately (34, 52).

Animals and immunizations. This study was carried out in strict accordance with the recommendations described in the Guide for the Care and Use of Laboratory Animals of the National Institutes of Health, the Office of Animal Welfare, and the United States Department of Agriculture (53). All animal work was approved by the Oregon Health & Science University (OHSU) Institutional Animal Care and Use Committee. The facilities at the Oregon National Primate Research Center (ONPRC) are accredited by the American Association for Accreditation of Laboratory Animal Care. *Macaca mulatta* (rhesus macaques) between 2 and 5 years of age were housed at the ONPRC in Beaverton, OR. Six macaques were coimmunized with HIV-1_{ZM53} gp120 gene-expressing plasmids and soluble V2-scaffold proteins at weeks 0, 8, and 20. At each coimmunization, a total of 36 μg of HIV-1_{ZM53} gp120 plasmid DNA was delivered epidermally using a particle-mediated epidermal delivery (PMED) device (Gene Gun, XR-1 research model, PowderMed, Oxford, UK), by administering 2 μg of the DNA vaccines coating 1-μm gold particles into each of 18 sites along the shaved abdomen and upper thighs, as previously described (54). Simultaneously with the DNA gp120 administration by Gene Gun, 100 μg each of three V2-scaffold protein immunogens were delivered intramuscularly (i.m.): V1V2(A244)-2J9C, V1V2(ZM53)-2F5K, and V1V2(ZM109)-TTB. Protein was formulated prior to injection with not more than 20% Adjuplex adjuvant (Sigma) (54). Regular blood sampling was performed every 2 weeks.

All three protein immunogens had previously been shown to bind to the V2q MAb PG9, with binding levels comparable to that of BG505 SOSIP.664 gp140 (36). V2p MAb binding was strong for V1V2(A244)-2J9C, moderate for V1V2(ZM53)-2F5K, and absent for V1V2(ZM109)-TTB (36). V1V2(A244)-2J9C was the most reactive with the V2i MAbs tested, while V1V2(ZM53)-2F5K and V1V2(ZM109)-TTB also exhibited strong binding by V2i MAbs, although the binding profile suggested that the fine V2i epitopes displayed by these immunogens are each unique.

Luminex binding assay. Assays were performed as previously described (36). For isotype-specific measurements, 100 μl/well of either mouse anti-rhesus IgG1 (0.2 μg/ml), IgG2 (1:500), or IgG3 (2.5 μg/ml) (NHP Reagent Resource) was incubated on the plate for 30 min at room temperature in the dark with shaking. After being washed twice with 100 μl/well of PBS-TBN (phosphate-buffered saline [pH 7.4], Tween 20 [0.02% vol/vol], bovine serum albumin [BSA; 0.1% wt/vol], NaN_3 [0.02% wt/vol]), samples were incubated with either 100 μl of biotinylated anti-mouse IgG (4 μg/ml; Sigma) or biotinylated anti-monkey IgG (2 μg/ml) for total IgG (Rockland) for 30 min at room temperature in the dark with shaking. Beads coupled with rhesus IgG1, IgG2, and IgG3 (4 μg/million beads) were run to rule out any cross-reactivity among isotypes (data not shown). GraphPad Prism 7.03 was used to generate titration curves.

Purification of V2-specific Abs from NHP plasma. *N*-hydroxy-succinimide (NHS)-activated agarose dry resin 33-mg columns (Thermo Scientific) were washed with PBS once and spun at 10,000 rpm for 1 min. One milligram of V1V2(ZM109)-1FD6 in 500 μl of PBS was added to each column, and columns were incubated with end-over-end rotation for 1 h at room temperature. Columns were centrifuged as described above and washed twice with 500 μl of PBS. Flowthrough was monitored for protein concentration. Remaining active sites were blocked by adding 1 M Tris, pH 7.4, with end-over-end rotation for 30 min at room temperature, and columns were washed again twice in PBS. Plasma samples (84 μl) from each of the six animals were pooled for each time point and loaded onto separate V1V2(ZM109)-1FD6 affinity columns. Columns were incubated with end-over-end rotation for 1 h at room temperature. Columns were centrifuged as described above and washed twice with 500 μl of PBS. V2-specifc Abs were eluted with 400 μl of elution buffer (Fisher) and neutralized immediately with 40 μl of 1 M Tris, pH 9. Eluted Abs were concentrated with an Amicon Ultra 0.5-ml 10K filter (Millipore) according to the manufacturer's protocol. All protein concentrations were measured with a NanoDrop spectrophotometer.

Replication-competent, fluorescently tagged HIV-1 (HIV-GFP). Plasmids (infectious molecular clones) for a clade B virus engineered to express GFP were obtained from Benjamin Chen (55). Virus was produced by standard transfection of 293T cells as described previously (55). Supernatant was centrifuged through a 20% sucrose gradient and virus was titrated by a standard quantitative p24 ELISA (Fisher) as described previously (56).

ADCP. The protocol for the ADCP assay was based on that by Ackerman et al. (57). For bead-based ADCP, 5 μg of V1V2(ZM53)-2F5K, V1V2(ZM109)-1FD6, or V1V2(ZM109)-TTB was biotinylated using EZ-Link Sulfo-NHS-LC-LC-biotin (Thermo Scientific) and then conjugated to 1-μm fluorescent neutravidin beads (Thermo) according to the manufacturer's instructions. Conjugated beads were washed and resuspended in 0.1% BSA-PBS to a working dilution of 1:100. A total of 9×10^5 beads were aliquoted per well in round-bottom 96-well plates. Plasma was titrated using 4-fold dilutions and added to beads, incubated for 2 h at 37°C, and washed. A total of 2.5×10^4 THP-1 cells (ATCC) were added to each well and were incubated overnight at 37°C. For virus-based ADCP, 150 ng/ml (p24 quantification) of GFP-HIV was aliquoted in 96-well plates. V2-affinity-purified Abs from pooled plasma were incubated with virus for 2 h at 37°C. Fifty thousand THP-1 cells were added and incubated for 2 h at 37°C. After incubation, plates were washed three times and incubated in Accutase cell detachment solution (Innovative Cell

Technologies) for 10 min at room temperature (to gently remove any surface-bound virus, as described in reference 58). Plates were washed once more with Accutase. Phagocytosis for both assays was measured by flow cytometry using an LSR Fortessa. ADCP scores were calculated as percent bead- or virus-positive cells × mean fluorescence intensity (MFI) of bead-positive cells. AUC was calculated from the titration curves as described above.

ADCC assay. Using the assay developed by Alpert et al. (59), ADCC measurements were made with $SHIV_{SF162P3}$-infected target cells as described previously (36). AUC was calculated from the titration curves as described above.

Virus capture assay. Plates were coated with 1 μg/ml of anti-monkey IgG goat antibody (Rockland Immunochemicals) in PBS (pH 7.4; Life Technologies) and incubated at 4°C overnight. Plates were washed twice with PBS-Tween 20 (0.1%; Life Technologies), followed by blocking with 5% milk in PBS for 1 h at 37°C. Titrated plasma in 1% milk was transferred to the virus capture assay plate and incubated for 1 h at 37°C. Plates were washed as described above and ZM53 pseudovirus, produced by a well-established protocol (60) representing ~500,000 relative light units (RLU) according to previous titration on TZM-bl cells, was added and plates were incubated for 4 h at 37°C. Plates were kept at 4°C overnight to be used for p24 quantification the following day.

Quantitative p24 ELISA. Immulon 4 plates (Fisher) were coated with 1 μg/ml of the p24-specific HIV MAb 241-D and kept at 4°C overnight. p24 ELISA and virus capture plates were washed six times. The p24 ELISA plate was blocked using 3% BSA (Life Technologies) in PBS, while the virus capture plate contents were lysed with 120 μl of 0.5% Triton X-100 in PBS for 1 h at 37°C. A p24 standard (Immune Technology) was diluted in lysis buffer. The blocked p24 ELISA plate was washed six times, followed by addition of the lysed captured pseudovirus and the p24 standard to the wells of the p24 ELISA plate, which was incubated for 1 h at 37°C. The plate was washed six times, followed by addition of 1 μg/ml of biotinylated p24-specific MAb 91-5 in 1% BSA-PBS. The plate was incubated and washed as described above, followed by addition of streptavidin-horseradish peroxidase (HRP) (Pierce) diluted 1:1,000 in 1% BSA-PBS and incubation as described above. Plates were washed, substrate solution was added (KPL), and plates were read at 450 nm by an ELISA plate reader.

SUPPLEMENTAL MATERIAL

Supplemental material is available online only.

SUPPLEMENTAL FILE 1, PDF file, 0.2 MB.

ACKNOWLEDGMENTS

The NIH/NIAID provided funding to all authors under grant number P01 AI100151. In addition, S. Zolla-Pazner was supported by funds from the Department of Medicine, Division of Infectious Diseases, Icahn School of Medicine at Mount Sinai.

REFERENCES

1. Haynes BF, Gilbert PB, McElrath MJ, Zolla-Pazner S, Tomaras GD, Alam SM, Evans DT, Montefiori DC, Karnasuta C, Sutthent R, Liao HX, DeVico AL, Lewis GK, Williams C, Pinter A, Fong Y, Janes H, DeCamp A, Huang Y, Rao M, Billings E, Karasavvas N, Robb ML, Ngauy V, de Souza MS, Paris R, Ferrari G, Bailer RT, Soderberg KA, Andrews C, Berman PW, Frahm N, De Rosa SC, Alpert MD, Yates NL, Shen X, Koup RA, Pitisuttithum P, Kaewkungwal J, Nitayaphan S, Rerks-Ngarm S, Michael NL, Kim JH. 2012. Immune-correlates analysis of an HIV-1 vaccine efficacy trial. N Engl J Med 366:1275–1286. https://doi.org/10.1056/NEJMoa1113425.
2. Rerks-Ngarm S, Pitisuttithum P, Nitayaphan S, Kaewkungwal J, Chiu J, Paris R, Premsri N, Namwat C, de Souza M, Adams E, Benenson M, Gurunathan S, Tartaglia J, McNeil JG, Francis DP, Stablein D, Birx DL, Chunsuttiwat S, Khamboonruang C, Thongcharoen P, Robb ML, Michael NL, Kunasol P, Kim JH, Investigators M-T, MOPH-TAVEG Investigators. 2009. Vaccination with ALVAC and AIDSVAX to prevent HIV-1 infection in Thailand. N Engl J Med 361:2209–2220. https://doi.org/10.1056/NEJMoa0908492.
3. Zolla-Pazner S, Edlefsen PT, Rolland M, Kong X-P, deCamp A, Gottardo R, Williams C, Tovanabutra S, Sharpe-Cohen S, Mullins JI, deSouza MS, Karasavvas N, Nitayaphan S, Rerks-Ngarm S, Pitisuttihum P, Kaewkungwal J, O'Connell RJ, Robb ML, Michael NL, Kim JH, Gilbert P. 2014. Vaccine-induced human antibodies specific for the third variable region of HIV-1 gp120 impose immune pressure on infecting viruses. EBioMedicine 1:37–45. https://doi.org/10.1016/j.ebiom.2014.10.022.
4. Zolla-Pazner S, deCamp A, Gilbert PB, Williams C, Yates NL, Williams WT, Howington R, Fong Y, Morris DE, Soderberg KA, Irene C, Reichman C, Pinter A, Parks R, Pitisuttithum P, Kaewkungwal J, Rerks-Ngarm S, Nitayaphan S, Andrews C, O'Connell RJ, Yang Z-y, Nabel GJ, Kim JH, Michael NL, Montefiori DC, Liao H-X, Haynes BF, Tomaras GD. 2014. Vaccine-induced IgG antibodies to V1V2 regions of multiple HIV-1 subtypes correlate with decreased risk of HIV-1 infection. PLoS One 9:e87572. https://doi.org/10.1371/journal.pone.0087572.
5. Ackerman M, Nimmerjahn F. 2014. Antibody Fc. Elsevier, San Diego, CA.
6. Yates NL, Liao H-X, Fong Y, deCamp A, Vandergrift NA, Williams WT, Alam SM, Ferrari G, Yang Z-y, Seaton KE, Berman PW, Alpert MD, Evans DT, O'Connell RJ, Francis D, Sinangil F, Lee C, Nitayaphan S, Rerks-Ngarm S, Kaewkungwal J, Pitisuttithum P, Tartaglia J, Pinter A, Zolla-Pazner S, Gilbert PB, Nabel GJ, Michael NL, Kim JH, Montefiori DC, Haynes BF, Tomaras GD. 2014. Vaccine-induced Env V1-V2 IgG3 correlates with lower HIV-1 infection risk and declines soon after vaccination. Sci Transl Med 6:228ra39. https://doi.org/10.1126/scitranslmed.3007730.
7. Chung AW, Ghebremichael M, Robinson H, Brown E, Choi I, Lane S, Dugast AS, Schoen MK, Rolland M, Suscovich TJ, Mahan AE, Liao L, Streeck H, Andrews C, Rerks-Ngarm S, Nitayaphan S, de Souza MS, Kaewkungwal J, Pitisuttithum P, Francis D, Michael NL, Kim JH, Bailey-Kellogg C, Ackerman ME, Alter G. 2014. Polyfunctional Fc-effector profiles mediated by IgG subclass selection distinguish RV144 and VAX003 vaccines. Sci Transl Med 6:228ra38. https://doi.org/10.1126/scitranslmed.3007736.
8. Tomaras GD, Ferrari G, Shen X, Alam SM, Liao HX, Pollara J, Bonsignori M, Moody MA, Fong Y, Chen X, Poling B, Nicholson CO, Zhang R, Lu X, Parks R, Kaewkungwal J, Nitayaphan S, Pitisuttithum P, Rerks-Ngarm S, Gilbert PB, Kim JH, Michael NL, Montefiori DC, Haynes BF. 2013. Vaccine-induced plasma IgA specific for the C1 region of the HIV-1 envelope blocks binding and effector function of IgG. Proc Natl Acad Sci U S A 110:9019–9024. https://doi.org/10.1073/pnas.1301456110.
9. Pollara J, Bonsignori M, Moody MA, Liu P, Alam SM, Hwang K-K, Gurley TC, Kozink DM, Armand LC, Marshall DJ, Whitesides JF, Kaewkungwal J, Nitayaphan S, Pitisuttithum P, Rerks-Ngarm S, Robb ML, O'Connell RJ, Kim JH, Michael NL, Montefiori DC, Tomaras GD, Liao H-X, Haynes BF,

Ferrari G. 2014. HIV-1 vaccine-induced C1 and V2 Env-specific antibodies synergize for increased antiviral activities. J Virol 88:7715–7726. https://doi.org/10.1128/JVI.00156-14.
10. Chung AW, Kumar MP, Arnold KB, Yu WH, Schoen MK, Dunphy LJ, Suscovich TJ, Frahm N, Linde C, Mahan AE, Hoffner M, Streeck H, Ackerman ME, McElrath MJ, Schuitemaker H, Pau MG, Baden LR, Kim JH, Michael NL, Barouch DH, Lauffenburger DA, Alter G. 2015. Dissecting polyclonal vaccine-induced humoral immunity against HIV using systems serology. Cell 163:988–998. https://doi.org/10.1016/j.cell.2015.10.027.
11. Tebo AE, Kremsner PG, Luty AJ. 2001. Plasmodium falciparum: a major role for IgG3 in antibody-dependent monocyte-mediated cellular inhibition of parasite growth in vitro. Exp Parasitol 98:20–28. https://doi.org/10.1006/expr.2001.4619.
12. Scharf O, Golding H, King LR, Eller N, Frazier D, Golding B, Scott DE. 2001. Immunoglobulin G3 from polyclonal human immunodeficiency virus (HIV) immune globulin is more potent than other subclasses in neutralizing HIV type 1. J Virol 75:6558–6565. https://doi.org/10.1128/JVI.75.14.6558-6565.2001.
13. Florese RH, Demberg T, Xiao P, Kuller L, Larsen K, Summers LE, Venzon D, Cafaro A, Ensoli B, Robert-Guroff M. 2009. Contribution of nonneutralizing vaccine-elicited antibody activities to improved protective efficacy in rhesus macaques immunized with Tat/Env compared with multigenic vaccines. J Immunol 182:3718–3727. https://doi.org/10.4049/jimmunol.0803115.
14. Hessell AJ, Hangartner L, Hunter M, Havenith CE, Beurskens FJ, Bakker JM, Lanigan CM, Landucci G, Forthal DN, Parren PW, Marx PA, Burton DR. 2007. Fc receptor but not complement binding is important in antibody protection against HIV. Nature 449:101–104. https://doi.org/10.1038/nature06106.
15. Chung AW, Isitman G, Navis M, Kramski M, Center RJ, Kent SJ, Stratov I. 2011. Immune escape from HIV-specific antibody-dependent cellular cytotoxicity (ADCC) pressure. Proc Natl Acad Sci U S A 108:7505–7510. https://doi.org/10.1073/pnas.1016048108.
16. Bournazos S, Klein F, Pietzsch J, Seaman MS, Nussenzweig MC, Ravetch JV. 2014. Broadly neutralizing anti-HIV-1 antibodies require Fc effector functions for in vivo activity. Cell 158:1243–1253. https://doi.org/10.1016/j.cell.2014.08.023.
17. Pegu A, Yang Z-Y, Boyington JC, Wu L, Ko S-Y, Schmidt SD, McKee K, Kong W-P, Shi W, Chen X, Todd J-P, Letvin NL, Huang J, Nason MC, Hoxie JA, Kwong PD, Connors M, Rao SS, Mascola JR, Nabel GJ. 2014. Neutralizing antibodies to HIV-1 envelope protect more effectively in vivo than those to the CD4 receptor. Sci Transl Med 6:243ra88. https://doi.org/10.1126/scitranslmed.3008992.
18. Julg B, Tartaglia LJ, Keele BF, Wagh K, Pegu A, Sok D, Abbink P, Schmidt SD, Wang K, Chen X, Joyce MG, Georgiev IS, Choe M, Kwong PD, Doria-Rose NA, Le K, Louder MK, Bailer RT, Moore PL, Korber B, Seaman MS, Abdool Karim SS, Morris L, Koup RA, Mascola JR, Burton DR, Barouch DH. 2017. Broadly neutralizing antibodies targeting the HIV-1 envelope V2 apex confer protection against a clade C SHIV challenge. Sci Transl Med 9:eaal1321. https://doi.org/10.1126/scitranslmed.aal1321.
19. Barouch DH, Liu J, Li H, Maxfield LF, Abbink P, Lynch DM, Iampietro MJ, SanMiguel A, Seaman MS, Ferrari G, Forthal DN, Ourmanov I, Hirsch VM, Carville A, Mansfield KG, Stablein D, Pau MG, Schuitemaker H, Sadoff JC, Billings EA, Rao M, Robb ML, Kim JH, Marovich MA, Goudsmit J, Michael NL. 2012. Vaccine protection against acquisition of neutralization-resistant SIV challenges in rhesus monkeys. Nature 482:89–93. https://doi.org/10.1038/nature10766.
20. Vaccari M, Gordon SN, Fourati S, Schifanella L, Liyanage NPM, Cameron M, Keele BF, Shen X, Tomaras GD, Billings E, Rao M, Chung AW, Dowell KG, Bailey-Kellogg C, Brown EP, Ackerman ME, Vargas-Inchaustegui DA, Whitney S, Doster MN, Binello N, Pegu P, Montefiori DC, Foulds K, Quinn DS, Donaldson M, Liang F, Loré K, Roederer M, Koup RA, McDermott A, Ma Z-M, Miller CJ, Phan TB, Forthal DN, Blackburn M, Caccuri F, Bissa M, Ferrari G, Kalyanaraman V, Ferrari MG, Thompson D, Robert-Guroff M, Ratto-Kim S, Kim JH, Michael NL, Phogat S, Barnett SW, Tartaglia J, Venzon D, Stablein DM, Alter G, Sekaly R-P, Franchini G. 2016. Adjuvant-dependent innate and adaptive immune signatures of risk of SIV acquisition. Nat Med 22:762–770. https://doi.org/10.1038/nm.4105.
21. Vaccari M, Gordon SN, Fourati S, Schifanella L, Liyanage NPM, Cameron M, Keele BF, Shen X, Tomaras GD, Billings E, Rao M, Chung AW, Dowell KG, Bailey-Kellogg C, Brown EP, Ackerman ME, Vargas-Inchaustegui DA, Whitney S, Doster MN, Binello N, Pegu P, Montefiori DC, Foulds K, Quinn DS, Donaldson M, Liang F, Loré K, Roederer M, Koup RA, McDermott A, Ma Z-M, Miller CJ, Phan TB, Forthal DN, Blackburn M, Caccuri F, Bissa M, Ferrari G, Kalyanaraman V, Ferrari MG, Thompson D, Robert-Guroff M, Ratto-Kim S, Kim JH, Michael NL, Phogat S, Barnett SW, Tartaglia J, Venzon D, Stablein DM, Alter G, Sekaly R-P, Franchini G. 2016. Corrigendum: adjuvant-dependent innate and adaptive immune signatures of risk of SIVmac251 acquisition. Nat Med 22:1192. https://doi.org/10.1038/nm1016-1192a.
22. Hessell AJ, Shapiro MB, Powell R, Malherbe DC, McBurney SP, Pandey S, Cheever T, Sutton WF, Kahl C, Park B, Zolla-Pazner S, Haigwood NL. 2018. Reduced cell-associated DNA and improved viral control in macaques following passive transfer of a single anti-V2 monoclonal antibody and repeated simian/human immunodeficiency virus challenges challenges. J Virol 92:e02198-17. https://doi.org/10.1128/JVI.02198-17.
23. Liao HX, Bonsignori M, Alam SM, McLellan JS, Tomaras GD, Moody MA, Kozink DM, Hwang KK, Chen X, Tsao CY, Liu P, Lu X, Parks RJ, Montefiori DC, Ferrari G, Pollara J, Rao M, Peachman KK, Santra S, Letvin NL, Karasavvas N, Yang ZY, Dai K, Pancera M, Gorman J, Wiehe K, Nicely NI, Rerks-Ngarm S, Nitayaphan S, Kaewkungwal J, Pitisuttithum P, Tartaglia J, Sinangil F, Kim JH, Michael NL, Kepler TB, Kwong PD, Mascola JR, Nabel GJ, Pinter A, Zolla-Pazner S, Haynes BF. 2013. Vaccine induction of antibodies against a structurally heterogeneous site of immune pressure within HIV-1 envelope protein variable regions 1 and 2. Immunity 38:176–186. https://doi.org/10.1016/j.immuni.2012.11.011.
24. Aiyegbo MS, Shmelkov E, Dominguez L, Goger M, Battacharya S, deCamp AC, Gilbert PB, Berman PW, Cardozo T. 2017. Peptide targeted by human antibodies associated with HIV vaccine-associated protection assumes a dynamic alpha-helical structure. PLoS One 12:e0170530. https://doi.org/10.1371/journal.pone.0170530.
25. Gorny MK, Pan R, Williams C, Wang X-H, Volsky B, O'Neal T, Spurrier B, Sampson JM, Li L, Seaman MS, Kong X-P, Zolla-Pazner S. 2012. Functional and immunochemical cross-reactivity of V2-specific monoclonal antibodies from HIV-1-infected individuals. Virology 427:198–207. https://doi.org/10.1016/j.virol.2012.02.003.
26. Spurrier B, Sampson J, Gorny MK, Zolla-Pazner S, Kong XP. 2014. Functional implications of the binding mode of a human conformation-dependent V2 monoclonal antibody against HIV. J Virol 88:4100–4112. https://doi.org/10.1128/JVI.03153-13.
27. Mayr LM, Cohen S, Spurrier B, Kong XP, Zolla-Pazner S. 2013. Epitope mapping of conformational V2-specific anti-HIV human monoclonal antibodies reveals an immunodominant site in V2. PLoS One 8:e70859. https://doi.org/10.1371/journal.pone.0070859.
28. Chung AW, Crispin M, Pritchard L, Robinson H, Gorny MK, Yu X, Bailey-Kellogg C, Ackerman ME, Scanlan C, Zolla-Pazner S, Alter G. 2014. Identification of antibody glycosylation structures that predict monoclonal antibody Fc-effector function. AIDS 28:2523–2530. https://doi.org/10.1097/QAD.0000000000000444.
29. Musich T, Li L, Liu L, Zolla-Pazner S, Robert-Guroff M, Gorny MK. 2017. Monoclonal antibodies specific for the V2, V3, CD4-binding site, and gp41 of HIV-1 mediate phagocytosis in a dose-dependent manner. J Virol 91:e02325-16. https://doi.org/10.1128/JVI.02325-16.
30. Walker LM, Phogat SK, Chan-Hui PY, Wagner D, Phung P, Goss JL, Wrin T, Simek MD, Fling S, Mitcham JL, Lehrman JK, Priddy FH, Olsen OA, Frey SM, Hammond PW, Kaminsky S, Zamb T, Moyle M, Koff WC, Poignard P, Burton DR, Protocol G Principal Investigators. 2009. Broad and potent neutralizing antibodies from an African donor reveal a new HIV-1 vaccine target. Science 326:285–289. https://doi.org/10.1126/science.1178746.
31. Doria-Rose NA, Bhiman JN, Roark RS, Schramm CA, Gorman J, Chuang G-Y, Pancera M, Cale EM, Ernandes MJ, Louder MK, Asokan M, Bailer RT, Druz A, Fraschilla IR, Garrett NJ, Jarosinski M, Lynch RM, McKee K, O'Dell S, Pegu A, Schmidt SD, Staupe RP, Sutton MS, Wang K, Wibmer CK, Haynes BF, Abdool-Karim S, Shapiro L, Kwong PD, Moore PL, Morris L, Mascola JR. 2016. New member of the V1V2-directed CAP256-VRC26 lineage that shows increased breadth and exceptional potency. J Virol 90:76–91. https://doi.org/10.1128/JVI.01791-15.
32. Sok D, van Gils MJ, Pauthner M, Julien JP, Saye-Francisco KL, Hsueh J, Briney B, Lee JH, Le KM, Lee PS, Hua Y, Seaman MS, Moore JP, Ward AB, Wilson IA, Sanders RW, Burton DR. 2014. Recombinant HIV envelope trimer selects for quaternary-dependent antibodies targeting the trimer apex. Proc Natl Acad Sci U S A 111:17624–17629. https://doi.org/10.1073/pnas.1415789111.
33. Walker LM, Huber M, Doores KJ, Falkowska E, Pejchal R, Julien JP, Wang SK, Ramos A, Chan-Hui PY, Moyle M, Mitcham JL, Hammond PW, Olsen OA, Phung P, Fling S, Wong CH, Phogat S, Wrin T, Simek MD, Koff WC,

Wilson IA, Burton DR, Poignard P, Protocol G Principal Investigators. 2011. Broad neutralization coverage of HIV by multiple highly potent antibodies. Nature 477:466–470. https://doi.org/10.1038/nature10373.
34. Jiang X, Totrov M, Li W, Sampson JM, Williams C, Lu H, Wu X, Lu S, Wang S, Zolla-Pazner S, Kong XP. 2016. Rationally designed immunogens targeting HIV-1 gp120 V1V2 induce distinct conformation-specific antibody responses in rabbits. J Virol 90:11007–11019. https://doi.org/10.1128/JVI.01409-16.
35. Zolla-Pazner S, Powell R, Yahyaei S, Williams C, Jiang X, Li W, Lu S, Wang S, Upadhyay C, Hioe CE, Totrov M, Kong X. 2016. Rationally designed vaccines targeting the V2 region of HIV-1 gp120 induce a focused, cross-clade-reactive, biologically functional antibody response. J Virol 90:10993–11006. https://doi.org/10.1128/JVI.01403-16.
36. Hessell AJ, Powell R, Jiang X, Luo C, Weiss S, Dussupt V, Itri V, Fox A, Shapiro MB, Pandey S, Cheever T, Fuller DH, Park B, Krebs SJ, Totrov M, Haigwood NL, Kong XP, Zolla-Pazner S. 2019. Multimeric epitope-scaffold HIV vaccines target V1V2 and differentially tune polyfunctional antibody responses. Cell Rep 28:877–895.e6. https://doi.org/10.1016/j.celrep.2019.06.074.
37. Julien J-P, Cupo A, Sok D, Stanfield RL, Lyumkis D, Deller MC, Klasse P-J, Burton DR, Sanders RW, Moore JP, Ward AB, Wilson IA. 2013. Crystal structure of a soluble cleaved HIV-1 envelope trimer. Science 342:1477–1483. https://doi.org/10.1126/science.1245625.
38. Lyumkis D, Julien JP, de Val N, Cupo A, Potter CS, Klasse PJ, Burton DR, Sanders RW, Moore JP, Carragher B, Wilson IA, Ward AB. 2013. Cryo-EM structure of a fully glycosylated soluble cleaved HIV-1 envelope trimer. Science 342:1484–1490. https://doi.org/10.1126/science.1245627.
39. Pancera M, Shahzad-Ul-Hussan S, Doria-Rose NA, McLellan JS, Bailer RT, Dai K, Loesgen S, Louder MK, Staupe RP, Yang Y, Zhang B, Parks R, Eudailey J, Lloyd KE, Blinn J, Alam SM, Haynes BF, Amin MN, Wang LX, Burton DR, Koff WC, Nabel GJ, Mascola JR, Bewley CA, Kwong PD. 2013. Structural basis for diverse N-glycan recognition by HIV-1-neutralizing V1-V2-directed antibody PG16. Nat Struct Mol Biol 20:804–813. https://doi.org/10.1038/nsmb.2600.
40. Pancera M, Zhou T, Druz A, Georgiev IS, Soto C, Gorman J, Huang J, Acharya P, Chuang GY, Ofek G, Stewart-Jones GB, Stuckey J, Bailer RT, Joyce MG, Louder MK, Tumba N, Yang Y, Zhang B, Cohen MS, Haynes BF, Mascola JR, Morris L, Munro JB, Blanchard SC, Mothes W, Connors M, Kwong PD. 2014. Structure and immune recognition of trimeric pre-fusion HIV-1 Env. Nature 514:455–461. https://doi.org/10.1038/nature13808.
41. Totrov M, Jiang X, Kong XP, Cohen S, Krachmarov C, Salomon A, Williams C, Seaman MS, Abagyan R, Cardozo T, Gorny MK, Wang S, Lu S, Pinter A, Zolla-Pazner S. 2010. Structure-guided design and immunological characterization of immunogens presenting the HIV-1 gp120 V3 loop on a CTB scaffold. Virology 405:513–523. https://doi.org/10.1016/j.virol.2010.06.027.
42. Karasavvas N, Billings E, Rao M, Williams C, Zolla-Pazner S, Bailer RT, Koup RA, Madnote S, Arworn D, Shen X, Tomaras GD, Currier JR, Jiang M, Magaret C, Andrews C, Gottardo R, Gilbert P, Cardozo TJ, Rerks-Ngarm S, Nitayaphan S, Pitisuttithum P, Kaewkungwal J, Paris R, Greene K, Gao H, Gurunathan S, Tartaglia J, Sinangil F, Korber BT, Montefiori DC, Mascola JR, Robb ML, Haynes BF, Ngauy V, Michael NL, Kim JH, de Souza MS, MOPH TAVEG Collaboration. 2012. The Thai phase III HIV type 1 vaccine trial (RV144) regimen induces antibodies that target conserved regions within the V2 loop of gp120. AIDS Res Hum Retroviruses 28:1444–1457. https://doi.org/10.1089/aid.2012.0103.
43. Crowley AR, Ackerman ME. 2019. Mind the gap: how interspecies variability in IgG and its receptors may complicate comparisons of human and non-human primate effector function. Front Immunol 10:697. https://doi.org/10.3389/fimmu.2019.00697.
44. Nguyen DC, Sanghvi R, Scinicariello F, Pulit-Penaloza J, Hill N, Attanasio R. 2014. Cynomolgus and pigtail macaque IgG subclasses: characterization of IGHG genes and computational analysis of IgG/Fc receptor binding affinity. Immunogenetics 66:361–377. https://doi.org/10.1007/s00251-014-0775-4.
45. Brown BK, Wieczorek L, Sanders-Buell E, Rosa Borges A, Robb ML, Birx DL, Michael NL, McCutchan FE, Polonis VR. 2008. Cross-clade neutralization patterns among HIV-1 strains from the six major clades of the pandemic evaluated and compared in two different models. Virology 375:529–538. https://doi.org/10.1016/j.virol.2008.02.022.
46. Wang S, Farfan-Arribas DJ, Shen S, Chou TH, Hirsch A, He F, Lu S. 2006. Relative contributions of codon usage, promoter efficiency and leader sequence to the antigen expression and immunogenicity of HIV-1 Env DNA vaccine. Vaccine 24:4531–4540. https://doi.org/10.1016/j.vaccine.2005.08.023.
47. Zolla-Pazner S, Cohen SS, Krachmarov C, Wang S, Pinter A, Lu S. 2008. Focusing the immune response on the V3 loop, a neutralizing epitope of the HIV-1 gp120 envelope. Virology 372:233–246. https://doi.org/10.1016/j.virol.2007.09.024.
48. Song H, Nie X, Basu S, Singh M, Cerny J. 1999. Regulation of VH gene repertoire and somatic mutation in germinal centre B cells by passively administered antibody. Immunology 98:258–266. https://doi.org/10.1046/j.1365-2567.1999.00874.x.
49. Yildiz O, Kalthoff C, Raunser S, Kuhlbrandt W. 2007. Structure of GlnK1 with bound effectors indicates regulatory mechanism for ammonia uptake. EMBO J 26:589–599. https://doi.org/10.1038/sj.emboj.7601492.
50. Zhang P, Du J, Sun B, Dong X, Xu G, Zhou J, Huang Q, Liu Q, Hao Q, Ding J. 2006. Structure of human MRG15 chromo domain and its binding to Lys36-methylated histone H3. Nucleic Acids Res 34:6621–6628. https://doi.org/10.1093/nar/gkl989.
51. Reeves PJ, Callewaert N, Contreras R, Khorana HG. 2002. Structure and function in rhodopsin: high-level expression of rhodopsin with restricted and homogeneous N-glycosylation by a tetracycline-inducible N-acetylglucosaminyltransferase I-negative HEK293S stable mammalian cell line. Proc Natl Acad Sci U S A 99:13419–13424. https://doi.org/10.1073/pnas.212519299.
52. McLellan JS, Pancera M, Carrico C, Gorman J, Julien J-P, Khayat R, Louder R, Pejchal R, Sastry M, Dai K, O'Dell S, Patel N, Shahzad-Ul-Hussan S, Yang Y, Zhang B, Zhou T, Zhu J, Boyington JC, Chuang G-Y, Diwanji D, Georgiev I, Kwon YD, Lee D, Louder MK, Moquin S, Schmidt SD, Yang Z-Y, Bonsignori M, Crump JA, Kapiga SH, Sam NE, Haynes BF, Burton DR, Koff WC, Walker LM, Phogat S, Wyatt R, Orwenyo J, Wang L-X, Arthos J, Bewley CA, Mascola JR, Nabel GJ, Schief WR, Ward AB, Wilson IA, Kwong PD. 2011. Structure of HIV-1 gp120 V1/V2 domain with broadly neutralizing antibody PG9. Nature 480:336–343. https://doi.org/10.1038/nature10696.
53. National Research Council. 2011. Guide for the care and use of laboratory animals, 8th ed. National Academies Press, Washington, DC.
54. Hessell AJ, Malherbe DC, Pissani F, McBurney S, Krebs SJ, Gomes M, Pandey S, Sutton WF, Burwitz BJ, Gray M, Robins H, Park BS, Sacha JB, LaBranche CC, Fuller DH, Montefiori DC, Stamatatos L, Sather DN, Haigwood NL. 2016. Achieving potent autologous neutralizing antibody responses against tier 2 HIV-1 viruses by strategic selection of envelope immunogens. J Immunol 196:3064–3078. https://doi.org/10.4049/jimmunol.1500527.
55. Hubner W, Chen P, Del Portillo A, Liu Y, Gordon RE, Chen BK. 2007. Sequence of human immunodeficiency virus type 1 (HIV-1) Gag localization and oligomerization monitored with live confocal imaging of a replication-competent, fluorescently tagged HIV-1. J Virol 81:12596–12607. https://doi.org/10.1128/JVI.01088-07.
56. McKeating JA, McKnight A, Moore JP. 1991. Differential loss of envelope glycoprotein gp120 from virions of human immunodeficiency virus type 1 isolates: effects on infectivity and neutralization. J Virol 65:852–860. https://doi.org/10.1128/JVI.65.2.852-860.1991.
57. Ackerman ME, Moldt B, Wyatt RT, Dugast AS, McAndrew E, Tsoukas S, Jost S, Berger CT, Sciaranghella G, Liu Q, Irvine DJ, Burton DR, Alter G. 2011. A robust, high-throughput assay to determine the phagocytic activity of clinical antibody samples. J Immunol Methods 366:8–19. https://doi.org/10.1016/j.jim.2010.12.016.
58. Gach JS, Bouzin M, Wong MP, Chromikova V, Gorlani A, Yu KT, Sharma B, Gratton E, Forthal DN. 2017. Human immunodeficiency virus type-1 (HIV-1) evades antibody-dependent phagocytosis. PLoS Pathog 13:e1006793. https://doi.org/10.1371/journal.ppat.1006793.
59. Alpert MD, Harvey JD, Lauer WA, Reeves RK, Piatak M, Jr, Carville A, Mansfield KG, Lifson JD, Li W, Desrosiers RC, Johnson RP, Evans DT. 2012. ADCC develops over time during persistent infection with live-attenuated SIV and is associated with complete protection against SIV(mac)251 challenge. PLoS Pathog 8:e1002890. https://doi.org/10.1371/journal.ppat.1002890.
60. Li M, Gao F, Mascola JR, Stamatatos L, Polonis VR, Koutsoukos M, Voss G, Goepfert P, Gilbert P, Greene KM, Bilska M, Kothe DL, Salazar-Gonzalez JF, Wei X, Decker JM, Hahn BH, Montefiori DC. 2005. Human immunodeficiency virus type 1 env clones from acute and early subtype B infections for standardized assessments of vaccine-elicited neutralizing antibodies. J Virol 79:10108–10125. https://doi.org/10.1128/JVI.79.16.10108-10125.2005.